Nonlinear Pattern Formation of Faraday Waves

Doug Binks and Willem van de Water
Physics Department, Eindhoven University of Technology, P.O. Box 513, 5600 MB, Eindhoven, The Netherlands
(Received 18 November 1996)

A cascade of surface wave patterns with increasing rotational symmetry ranging from simple square to tenfold quasiperiodic is observed for Faraday waves. The experiment concerns the excitation of subharmonic standing surface waves by oscillating vertical acceleration. Our observation agrees with the prediction of a recent theory. By presenting these predictions in a dimensionless form, we illustrate the genericity of this phenomenon and emphasize the very favorable agreement with experiment. [S0031-9007(97)03210-9]

PACS numbers: 47.35+i, 47.54.+r

The Faraday-wave experiment concerns a free fluid surface undergoing oscillatory vertical acceleration [1,2]. When the amplitude of the excitation exceeds a critical value, standing wave patterns are formed on the surface which oscillate at half the frequency of the drive [3]. For large enough containers, the surface pattern becomes approximately independent of the boundaries, and line, square, hexagonal, triangular, and 8-fold quasiperiodic patterns have been observed [4–6]. However, despite this profusion of observed patterns a cohesive picture has not emerged.

In a recent paper Zhang and Viñals [7] derived an equation describing the slow evolution in space and time of standing Faraday-wave amplitudes in the weakly damped and infinite depth limit. This theory predicts the preferred pattern at onset as the one that minimizes a Lyapunov functional. For most excitation frequencies a square pattern is predicted, in agreement with previous experiments in low viscosity fluids. In a narrow frequency interval, however, the emergence of n-fold rotationally symmetric patterns was predicted, such as hexagons ($n = 3$), 8-fold quasiperiodic patterns ($n = 4$), and so forth. All patterns with $n > 2$ are predicted to occur for long wavelengths, and for low dissipation, requiring verification in a large experiment. Below, we will precisely quantify the "size" of the experiment. In this Letter we present for the first time quantitative experimental evidence which supports this theory. Using slow automated scans of the parameters in a large experiment, we have observed a cascade of patterns with symmetries that range from $n = 2$ (squares), $n = 3$ (triangles), to $n = 4$ and 5 (8- and 10-fold quasipatterns). By presenting the predictions of this theory in dimensionless form, we illustrate the genericity of the observed cascade of rotational symmetries and the very favorable agreement between theory and experiment.

Our experiment consists of a 440 mm diameter sealed circular container with a vertical wall boundary filled to a height of 20 mm with the working fluid [8]. The bottom of the container is a 2 cm thick glass plate; it is attached to a hollow conical structure at approximately 2/3 of its radius to suppress the lowest vibration mode of the plate. The entire structure is mounted on top of an electromagnetic exciter that can deliver a maximum force of 2900 N. The acceleration amplitude is measured by means of piezoelectric accelerometers with one high resolution sensor mounted to the bottom center of the cone, and two lightweight sensors which may be mounted at various positions on the container. Using phase-sensitive averaging of the sensors' output, a precise measure of the acceleration and its inhomogeneity could be obtained. By carefully designing the construction, we have moved the lowest resonant mode of joint vibration of cone and container to ≈ 700 Hz. In the frequency range of interest (25–45 Hz) the major contribution to acceleration inhomogeneity is side-to-side motion of the exciter as a whole. The measured acceleration inhomogeneity over the plate is less than 2%. The amplitude of the exciter is controlled to better than 0.2%, and the frequency is constant to 1 part in 10^6.

The waves are visualized using the refraction at the surface of the fluid of parallel light incident from below. Unlike other visualization techniques [4,5], this method allows discrimination between wave minima and wave maxima. Images of the surface are made using a high resolution CCD camera with a liquid crystal shutter. A programmable hardware system allows us to control the phase of the excitation at which the image is taken. The integration time of the image is kept well below half the oscillation period of the wave, so that the image can be considered as an instantaneous snapshot of the surface.

At onset, the wavelength is to a good approximation given by the inviscid deep fluid dispersion relation

$$g_*(1 + k_*^2) = 1\,, \tag{1}$$

where $g_* = gk/\omega^2$ with g the acceleration due to gravity, k the wave number, and 2ω the excitation frequency. The wave number k_* is nondimensionalized as $k_* = k\sqrt{\alpha/\rho g}$, with α the surface tension and ρ the density of the fluid. The measured wavelength agrees with the dispersion relation from 25–100 Hz to better than 1% (lower and higher frequencies could not be measured due to experimental difficulties). As will be explained later, this agreement is crucial for comparison with theory. The onset amplitude can be computed numerically using the

method of Kumar and Tuckerman [9]. At the frequencies of interest, measured onset accelerations are 10% higher than predicted. As a 1% agreement is reached at higher frequencies, we ascribe the discrepancy to the neglect of sidewall damping [10]. An important parameter is the dimensionless dissipation $\gamma = 2\nu k^2/\omega$ (an inverse Reynolds number). The theory is derived for $\gamma \ll 1$; for the experimental results discussed here $\gamma < 0.03$.

Figure 1 shows the surface of the fluid layer at frequencies where square ($n = 2$), hexagonal ($n = 3$), 8-fold quasiperiodic ($n = 4$), and 10-fold quasiperiodic ($n = 5$) emerge close to onset. Only part of the surface is imaged; the actual surface diameter is approximately twice that of the image's. These patterns are found in frequency ranges which agree with those theoretically predicted to within 10%. The images of the $n = 2, 3, 4$ patterns show a clear long-range orientational order, with minor defects which manifest as a slow bend in the case of the square pattern, and the appearance of triangularlike structures in the case of $n = 3$. These apparent triangles are the result of a π phase defect, as the alteration of hexagons and triangles can be reversed by shifting the phase at which the image is taken by π. For the 8-fold quasiperiodic pattern, there appears to be a point defect in the top central portion of the image. The ordering of the 10-fold pattern is only strong in the central region, although some 10-fold orientational order can be observed throughout the image.

Pattern formation at a reduced amplitude ϵ above onset is described by a nonlinear equation for the slow temporal variation of waves with amplitude A_j and wave vector $\mathbf{k}_j$ that interact with n other waves:

$$\frac{dA_j}{dt} = \epsilon A_j - \sum_{l=1}^{n} g(\theta_{jl})|A_l|^2 A_j\,, \qquad (2)$$

where θ_{jl} is the angle between wave vectors $\mathbf{k}_l$ and $\mathbf{k}_j$, which for neighboring wave vectors is π/n. While the form of the equation is generic for systems of the same symmetry, deriving the function $g(\theta_{jl})$ is highly nontrivial. It is precisely this which Zhang and Viñals [7] have achieved in the small dissipation limit $\gamma \ll 1$. Equation (2) is of gradient form $\partial_t A_j = -\partial \mathcal{F}_n/\partial A_j^*$, and the symmetry of the preferred pattern is that for which the Lyapunov functional $\mathcal{F}_n$ is lowest. As system parameters (for example, the frequency) are varied, curves $\mathcal{F}_{n'}$ at a different $n' \neq n$ may cross $\mathcal{F}_n$ and the pattern with n' becomes prefered instead. Thus, the regions in frequency space can be found where a given symmetry emerges at onset.

In order to find the regions of stability of patterns with a given symmetry in the experiment, we have performed a set of quasistatic amplitude scans from just below the critical amplitude a_c to $\varepsilon = a/a_c - 1 = 0.2$ above (where a_c is the experimental amplitude at which waves first appear), over a range of frequencies. The amplitude is increased in steps of $\approx 1\%$, then held for 2000 s after which images are taken for the next 1000 s to observe any temporal dependence. The images were analyzed in an automatic fashion using a correlation technique that is described below. The experimental phase diagram is shown in Fig. 2. The measured points are on the stability boundary of a given pattern when the excitation amplitude

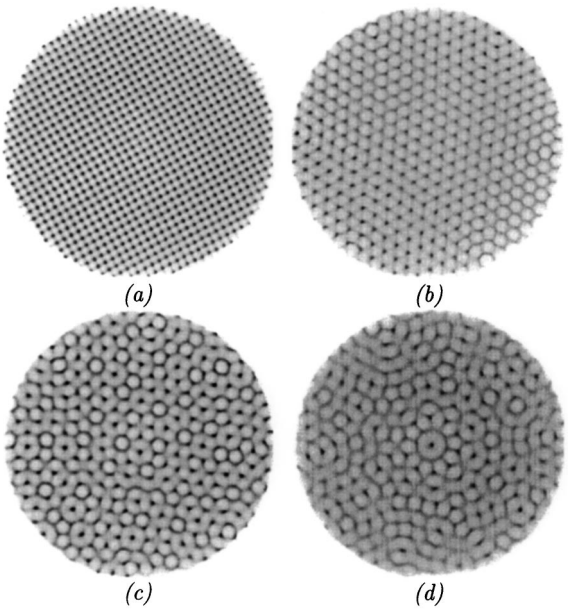

FIG. 1. Images of the fluid surface at frequencies f where patterns of square symmetry are observed: (a) $f = 45.0$ Hz, hexagonal symmetry; (b) $f = 30.0$ Hz, 8-fold quasiperiodic; (c) $f = 29.0$ Hz, and 10-fold quasiperiodic; (d) $f = 27.0$ Hz. The visualized region is of diameter 26 cm, approximately 1/2 the diameter of the container.

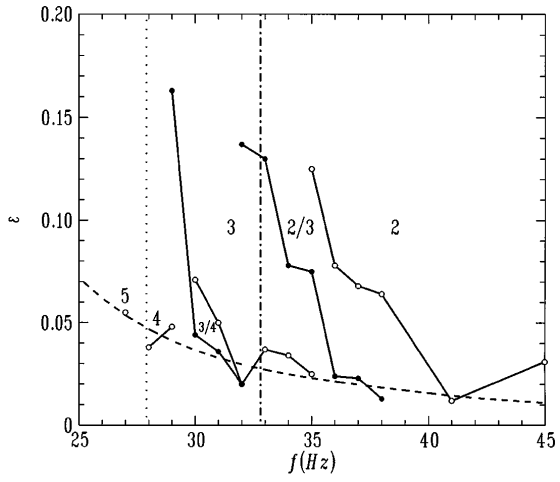

FIG. 2. Stability diagram of observed $2n$-fold symmetric patterns. Open circles: excitation amplitude ε above which a $2n$-fold stationary pattern is observed in an upward scan of ε. Closed dots: excitation amplitude above which a pattern of mixed symmetry $2n/2(n+1)$ is observed. Dotted line: predicted transition $n = 3 \rightarrow 4$; dash-dotted line: predicted trasition $n = 2 \rightarrow 3$. Dashed line: excitation amplitude where the computed width Δk of neutrally stable tongues equals π/L, where L is the diameter of the container ($L = 44$ cm).

is increased slowly. Apart from the $n = 2, 3, 4$, and 5 stationary patterns, also patterns with mixed behavior were found. In these patterns either oscillations from one rotational symmetry to the other or the simultaneous occurrence of both symmetries in a single pattern was found. The 10-fold quasiperiodic pattern was observed over a very small region of parameter space, both in frequency and excitation amplitude. We have also plotted vertical lines where the theoretically predicted boundaries for $n = 2$ to $n = 3$, and $n = 3$ to $n = 4$ occur. Favorable agreement is found at $\varepsilon > 0.1$, with the mixed pattern behavior consistent with the bicritical point. Interestingly, this value of ε is where the strongest patterns, such as those in Fig. 1, are found. The theory does not predict the $n = 5$ 10-fold quasiperiodic pattern; however, the calculated $\mathcal{F}_4$ and $\mathcal{F}_5$ Lyapunov functionals come very close in the region where the $n = 5$ pattern is observed. We will argue below that this discrepancy is consistent with the neglect of a term $\mathcal{O}(\gamma^{3/2})$ in the theory.

The onset of the $2n$-fold symmetric patterns is found to be slightly offset from the $\varepsilon = 0$ line. Below these onset values, but above $\varepsilon = 0$, the surface deformation appears as either a simple Bessel mode or the sum of a low number of Bessel modes. In a finite system, rigid boundary conditions force the permissible wave vectors to be discrete. At the theoretical onset $\epsilon = 0$ (which is for an infinite system), the critical wave number k_c as given by the dispersion relation does not in general match with one of the permissible wave vectors. However, as ϵ is increased a band $\Delta k \propto \epsilon^{1/2}$ of wavenumbers becomes unstable. Onset in a one-dimensional finite system is observed when ϵ is large enough that Δk becomes the mode spacing π/L; the surface will then definitely become unstable. Taking this argument to the two-dimensional case is complicated by the much larger density of states in two dimensions which allows onset before $\Delta k \approx \pi/L$. However, when $\Delta k = \pi/L$ any rotational symmetry of the standing wave pattern should become possible, irrespective of the boundary condition. In Fig. 2 we have plotted the line $\Delta k = \pi/L$ (using $\varepsilon \approx \epsilon$) calculated using the numerical approach of Kumar and Tuckerman [9]. The onset of the n-wave patterns lies close to this curve, although the most regular patterns are found at $\varepsilon \approx 0.1$.

In order to detect the symmetry of the observed surface states in a semiautomatic fashion, we first computed a 2-dimensional power spectrum of each pattern. An n-fold symmetric pattern will have $2n$ peaks in its power spectrum on a circle with radius k. In order to bring out the regular spacing of the peaks more clearly, we have computed from each power spectrum $p(k, \theta)$, the angular correlation function $C(\phi)$ averaged over a band of wave numbers of width $\approx k$

$$C(\phi) = \left\langle \frac{\sum_\theta [p(k,\theta) - \overline{p}][p(k,\theta + \phi) - \overline{p}]}{\sum_\theta [p(k,\theta) - \overline{p}]^2} \right\rangle. \quad (3)$$

In comparison with other methods [5], the resulting function $C(\phi)$ will for an n-fold pattern have peaks at precisely $2\pi/n$, independent of the orientation of the pattern and the k range over which $C(\phi)$ is averaged. This last point is crucial, as harmonics can lead to extra peaks in $C(\phi)$ if $p(k, \theta)$ is summed over k before computing $C(\phi)$. As an example we show in Fig. 3 the function $C(\phi)$ for the states that are encountered in a slow upward scan of ε at $f = 35$ Hz (see also Fig. 2). For each amplitude ε, $C(\phi)$ was averaged over five images that were taken 200 s apart. Figure 3 shows the transition from the flat state below onset to the hexagonal state with peaks at 60° and 120°, which in turn gives way to the square state with a peak at 90°. It is interesting to note that the hexagonal state develops at a value of ε where $\Delta k = \pi/L$. When the hexagonal state disappears, individual snapshots of the surface show oscillating hexagons and squares. The square state has the sharpest peak at $\varepsilon \approx 0.15$; above this excitation amplitude defects appear in the surface which separate domains of different orientation.

Surface waves are governed by four dimensionless parameters, k_*, g_*, γ, and ε. The first two are coupled through the dispersion relation [Eq. (1) or its viscous equivalent [11]], so that at onset ($\varepsilon = 0$) pattern formation is determined by two parameters, say k_* and γ. It is very instructive to draw the stability regions of $2n$-fold symmetric patterns in the γ, k_* plane. The result is shown in Fig. 4 which was computed using the Lyapunov functionals $\mathcal{F}_n$ that are given by Zhang and Viñals [7]. The phase diagram shows only the area of parameter space for which $k_* < 1$ and $\gamma < 0.1$, corresponding to low dissipation gravity waves. Outside this region only the $n = 2$ square state was found, in agreement with low dissipation

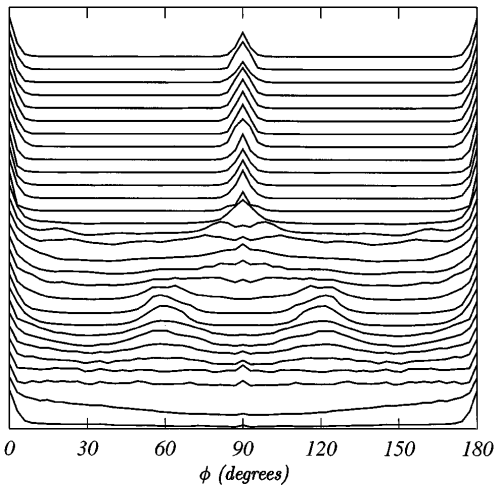

FIG. 3. Angular correlation $C(\phi)$ of Fourier-transformed images of the fluid surface. The images were taken at 35 Hz and reduced excitation amplitudes $\varepsilon = -0.01$ (lowest curve) to $\varepsilon = 0.23$ (highest curve). Two regions of well-defined symmetry can be observed, the first with peaks at 60° and 120° corresponding to $n = 3$ (hexagonal state) and the second with a peak at 90° corresponding to $n = 2$ (square state). The intervening region is a mixed $n = 2/3$ phase.

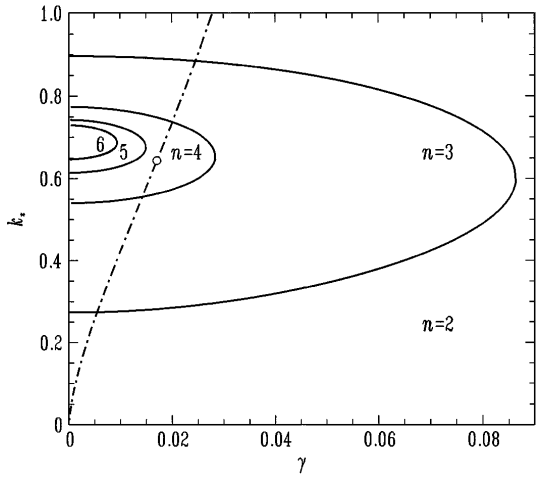

FIG. 4. Stability diagram of the $2n$-fold symmetric patterms in the γ, k_* plane. Patterns with $2n$-fold rotational symmetry are stable inside an infinite series of nested stability regions; they are drawn (full lines) for n up to $n = 6$. The stability regions converge to the point $\gamma = 0$, $k_* = \sqrt{1/2}$. Dash-dotted line: path followed by our experiment when the excitation frequency is varied; the lowest frequency in Fig. 2 corresponds to the open circle.

capillary wave experiments (lines are found for high dissipation experiments; however, this is beyond the range of validity of this theory). A sequence of n-wave regions consecutively enclosing $n + 1$-wave regions is observed, with the stability boundaries rapidly asymptoting to the point $\gamma = 0$, $k_* = \sqrt{1/2}$. In addition to the stability boundaries, we have plotted the line through this parameter space which our experiment follows as the excitation frequency is varied with increasing frequency corresponding to increasing γ and k_*. The choice of fluid parameters in our experiment causes this path to cross the $n = 2, 3,$ and 4 stability regions and to come close to the $n = 5$ boundary. The experimentally observed boundaries for $n = 2, 3, 4,$ and 5 are within 10% of the predicted boundaries, though the experimental path does not actually cross the predicted $n = 5$ boundary. We argue that this discrepancy may be reconciled by the consideration of the next higher order term $\gamma^{3/2}$ in the theory. In [7] γ enters the function $g(\theta)$ through its equation to the nondimensional onset acceleration $a_* = ak/4\omega^2 = \gamma$. However, Müller *et al.* [11] find that the next higher order correction to a_* is $a_* = \gamma - \gamma^{3/2}/2$. Taking this correction into account shifts the boundaries in Fig. 4 by $\gamma^{3/2}/2$ to higher dissipation. In our case this shift is ≈ 0.09, and very favorable agreement with the experiment is obtained. By using a lower visosity silicon oil, it should be possible to cross the $n = 6$ or higher boundaries, though a larger experiment would be required.

A fundamental ingredient of the theory by Zhang and Viñals [7] is a three-wave resonance phenomenon where two waves with angular separation θ_r to each other interact to produce a third wave which satisfies the dispersion relation Eq. (1) at 2ω. Standing waves with angular separation close to θ_r will not be favored as they will lose energy to the wave at 2ω. This resonance phenomenon is reflected in the coupling function $g(\theta)$ [Eq. (2)] which is large near θ_r. The cascade of patterns with increasing symmetry depends in a delicate way on the behavior of $g(\theta)$, which in turn is determined by the three-wave resonance phenomenon. As this resonance phenomenon is crucially dependent on the validity of the deep fluid dispersion relation [Eq. (1)], precise satisfaction of this relation is a first experimental requirement for the observation of the predicted patterns. We expect, therefore, that experiments in shallow fluid layers where the deep fluid dispersion relation is invalid will show different phenomena than those reported in the present Letter [5].

In conclusion, we have demonstrated the existence of a cascade of periodic and quasiperiodic patterns with increasing rotational symmetry near to a special resonance point. This highly nontrivial course of events appears to be remarkably well described by a recent theory.

We thank Reinout Dekkers, Kristian Schaadt, and Gerard Trines for technical assistance, and Eric Bosch, Hanns Walter Müller, Laurette Tuckerman, Christian Wagner, and Mark Westra for many useful discussions. We gratefully acknowledge financial support by the "Nederlandse Organisatie voor Wetenschappelijk Onderzoek (NWO)".

[1] M. Faraday, Philos. Trans. R. Soc. London **121**, 319 (1831).
[2] M. C. Cross and P. Hohenberg, Rev. Mod. Phys. **65**, 851 (1993).
[3] T. B. Benjamin and F. Ursell, Proc. R. Soc. London A **255**, 505 (1954).
[4] K. Kumar and K. M. S. Bajaj, Phys. Rev. E **52**, R4606 (1995).
[5] A. Kudrolli and J. P. Gollub, Physica D **97**, 133 (1996).
[6] B. Christiansen, P. Alstrom, and M. T. Levinson, Phys. Rev. Lett. **68**, 2157 (1992).
[7] W. Zhang and J. Viñals, Phys. Rev. E **53**, R4286 (1996).
[8] The large depth is necessary to ensure agreement with the theory which is derived in the infinite depth limit. The working fluid is temperature controlled at 21.00 ± 0.05 °C. The fluid is a low viscosity, low surface tension silicon oil with (at 21.0°C) viscosity $\nu = 3.397 \times 10^{-6}$ m s^{-12}, density $\rho = 892.4$ kg m^{-3}, and surface tension $\alpha = 18.3 \times 10^{-3}$ J m^{-2}. The tendencies of the parameters with temperature are such that with they are constant to within 0.1%.
[9] K. Kumar and L. S. Tuckerman, J. Fluid Mech. **279**, 49 (1994).
[10] J. Bechhoefer, V. Ego, S. Manneville, and B. Johnson, J. Fluid Mech. **288**, 325 (1995).
[11] H. W. Müller, H. Wittmer, C. Wagner, J. Albers, and K. Knorr, Phys. Rev. Lett. **78**, 2357 (1997).